Journal of Metals, Materials and Minerals, 36(4), e2501, 2026

Epipremnum aureum silver nanoparticles: Antioxidant, antibacterial, and photocatalytic potentials

Venujan PRAKASH[1], Mathivathani KANDIAH[1,*], Beneli GUNARATNE[1], and Ominda PERERA[1]

[1] *Faculty of Life and Medical Sciences, BMS Campus, 591, Galle Road Colombo 06, Sri Lanka*

***Corresponding author e-mail**: mathi@bms.ac.lk

Received date:
2 September 2025
Revised date:
29 March 2026
Accepted date:
5 June 2026

Keywords:
Silver nanoparticle;
Epipremnum aureum;
Antioxidant;
Photocatalysis;
Antibacterial

Abstract

The rising concerns in medical industries and environmental remediation have prompted increased research in nanotechnology specifically green-synthesized silver nanoparticles (AgNPs) which use commonly available plant species for synthesis. This is environmentally friendly and sustainable, giving solutions to the current problems. This study investigates AgNP synthesis using *Epipremnum aureum* leaves (Golden, Neon, Jade, Marble-Queen, and Manjula), highlighting their promising applications by evaluating the antioxidant, photocatalytic, and antibacterial qualities. The synthesis under different temperatures and time showed optimum conditions as 60°C for 60 min. The scanning electron microscopy analysis showed 70 nm to 90 nm cubic Marble Queen_AgNP, Energy-dispersive X-ray analysis showed 74.1% Ag at 3 keV, zeta potential showed –25.3 mV, dynamic light scattering showed 74.61 nm and polydispersity index of 0.278, and Fourier transform infrared showed functional groups necessary for capping and stability of AgNPs. The photocatalytic impact of different concentrations of Marble Queen_AgNP was assessed using methyl red under different conditions: in the absence and presence of sunlight and with the addition of the catalyst. Upon the addition of a catalyst, 4000 ppm Marble-Queen demonstrated a rapid rate of degeneration of $k = 0.1948\ min^{-1}$ and a slower degradation rate of $0.0752\ min^{-1}$ with 266 ppm. The determination of antibacterial activity was performed by *Escherichia coli* and *Staphylococcus aureus*, in which higher activity was seen against *Escherichia coli*. The findings highlight that *Epipremnum aureum*_AgNPs hold promise in the advancement of eco-friendly approaches in the medicinal industry, environmental remediation, and antibacterial therapy.

1. Introduction

Currently, using green chemistry to improve and preserve our environment has been of the utmost importance. Through the path of nanotechnology, which arose in the mid-20th century from the principle of sciences and engineering, a more promising approach to generating new fields in biomedical sciences has been made possible in a variety of research fields. It's currently one of the most important areas for investment in modern science due to the concepts' quick development as well as the depth of their applications that impact every aspect of human life [1]. Therefore, the subject of nanotechnology presents opportunities for numerous industrial and medical exploits, particularly in the areas of therapeutics, equipment, and health [2]. Nanoparticles are microscopic particles that fall within the nanoscale (1 nm to 100 nm) [3], and they can be produced by different metals such as gold, silver, copper, zinc and titanium depending on the necessity. Among these metal nanoparticles, silver nanoparticles (AgNPs) with different size ranges are commonly synthesised due to their wide range of applications, such as in wastewater remediation, food packaging, cosmetics and biosensors. The synthesis can be achieved by various techniques such as physical, chemical, and biological/green [4,5]. Apart from their versatile applications, AgNPs are reported to have a high surface-to-volume ratio, strong chemical reactivity, and unique optical properties, which have led to their widespread use in recent years [6]. Furthermore, AgNPs have also been shown to be less harmful to mammalian cells than other nanoparticles [7].

The physical method utilizes the top-down approach where the nanoparticles are synthesized from a source or a bulk material, and the chemical and biological methods utilize the bottom-up method where the nanoparticles are produced from their atomic state. The physical and chemical method uses higher energy and produces toxic by-products that cause harm to the environment [8]. Interestingly, using ecologically friendly alternatives like microorganisms, enzymes, plants, or their extracts is the most effective way to produce nanoparticles. Green processing is quick, dependable, stable, and advantageous economically [9,10]. This is particularly applicable for plant extracts, which use their constituent biomolecules to reduce and stabilize metal ions [11,12].

Epipremnum aureum (*E. aureum*), also known as Golden pothos, belongs to the family Araceae and is native to Southeast Asia [13]. In Sri Lanka, this plant is a commonly grown houseplant as a hanging basket crop and is identified to have different varieties such as Neon, Marble Queen, Jade Pothos and N'Joy. This plant can become an invasive species when introduced to other tropical countries such as Sri Lanka, where it is not native. In Sri Lanka, this plant has not been used for studies in the field of nanotechnology; instead, it is used for crop cultivation or agricultural studies [14–16]. Research on this plant has documented the presence of phytochemicals or secondary metabolites such as alkaloids, steroidal terpenoids, cardiac glycosides, proteins, flavonoids, and phenols. These phytochemicals are responsible for the various medicinal uses of the *E. aureum* plant, such as antimicrobial, anti-inflammatory, and anti-cancer activities and detoxification [17, 18]. In the field of nanotechnology, *E. aureum* has shown growing potential in the synthesis of nanoparticles due to its vast phytochemical profile and medicinal uses. At present, *E. aureum* leaves have been utilised to synthesise AgNPs for screening as a potential anti-cancer agent [19–21], for copper sensing and antibacterial potential [22], and for potential in DNA interaction mechanisms due to phytochemicals present [23]. *E. aureum* leaves have been reported to also have potential in other nanoparticles such as zinc oxide and copper oxide nanoparticles [24-26]. These studies highlight the potential of *E. aureum* leaves in forming nanoparticles aided by phytochemicals present in the plant. Although previous studies have been conducted on AgNP synthesis by *E. aureum* leaves and its potential in different fields of science, research has not focused on different *E. aureum* leaf varieties. Therefore, the present study focuses on the green synthesis of AgNPs by five varieties of *E. aureum* leaves: Golden, Neon, Jade, Marble Queen and Manjula, found commonly in Sri Lanka, to investigate the effects of different phytochemicals on the AgNP synthesis process.

Nowadays, oxidative stress-related diseases are becoming a major health concern, such as diabetes, Alzheimer's and Parkinson's conditions [27]. Oxidative stress is a condition that occurs when an excess of oxidants, such as reactive oxygen or nitrogen species, disrupts the balance between an organism's antioxidative defense mechanisms and oxidants. The oxidants cause oxidative stress in cells, resulting in damage and, ultimately, accelerating cellular death [28]. The most significant class of oxidants, including radicals and non-radicals, are reactive oxygen species [29]. However, oxidants are opposed by antioxidants, which are natural or synthetic substances that may prevent or delay cell damage caused by oxidants. AgNPs also have the ability to act as an antioxidant, where according to the reaction condition, the produced AgNPs may be able to quench free radicals by either donating or accepting electrons. The chemical composition of the extract used to produce the AgNPs can affect this property, which typically gets improved as the AgNPs concentration rises. Additionally, because of their ability to interact with phenolic and flavonoid-rich extracts, AgNPs exhibit a significant radical-scavenging activity [30–32].

Antibiotic-resistant microbes have emerged as a result of the widespread use of antibiotics worldwide, contributing to an increasing health concern. According to reports, the prescribed antibiotics do not metabolize in the body, and when they are disposed of improperly, they result in contaminated water sources. Antibiotic residues encourage the development of bacterial resistance during wastewater treatment [33]. As a strategy to handle this antimicrobial resistance, the application of nanoparticles in a variety of sectors, including medical and food packaging, has been researched [34]. It has been reported that AgNPs derived from plants can broadly regulate the growth, reproduction, and pathogenicity of both gram-negative (G^-) and gram-positive (G^+) bacteria without causing resistance in them. [35]. They disrupt the bacterial cell wall by pore formation or diffusion through porins and induce oxidative stress, killing the bacteria inside out, and these multiple attack pathways prevent bacteria from adapting to them and building resistance [36,37].

In addition to this health matter, untreated azo dye discharge from paper, leather, cosmetics, and food-processing industries is a growing environmental problem. These dyes are characterised by the presence of one or more azo groups (–N=N–) in their structural composition [38–40], and common examples of frequently utilised azo dyes include methylene blue, methyl red, methyl orange, and congo red [41]. These dyes have high stability, resistance to light, and high chemical versatility, which affects their degradation process [42]. In particular, methyl red (MR) is classified as an acidic or monoazo dye having a molecular weight of 269.3 $g \cdot mol^{-1}$, low water solubility, a carboxyl functional group connected to a benzene ring, and one chromophore group (–N=N–) [43]. Finding safe and efficient methods for its environmental degradation is crucial given its toxicity and persistence in the environment [44]. Microbial degradation is one of the proposed degradation methods. However, this method's effectiveness depends on many parameters such as pH, temperature, and type of dye [45]. The need for the most ideal conditions and the production of toxic aromatic amines in the degradation process can cause acute toxicity to humans via the routes of oral or inhalation. Therefore, a sustainable degradation method should be developed to degrade these toxic azo dyes into non-toxic by-products and help minimise the impact on human health [46–48]. Metal nanoparticles such as coconut coir copper oxide nanoparticles [49], bamboo copper oxide nanoparticles [50], water hyacinth zinc oxide nanoparticles [51], and Peepal leaves cerium oxide nanoparticles [52] are known for their ability to degrade these dyes under the influence of light irradiation. Compared to other traditional techniques, AgNPs and their composites have a larger surface area than other toxic nanoparticles, are more effective as catalysts in the dye degradation processes and produce non-toxic byproducts [53]. Specifically, their surface plasmon resonance (SPR) phenomenon, which produces radicals, can target the azo bonds, enabling photocatalytic dye degradation [54].

The purpose of this study is to evaluate the antioxidant, photocatalytic, and antibacterial properties of AgNPs synthesized using five different types of *E. aureum* leaf extracts. The evaluation of antioxidant activity will be conducted by Total Flavonoid Content (TFC), Total Phenolic Content (TPC), and Total Antioxidant Content (TAC) assays. The photocatalytic activity will be investigated under various conditions using MR dye, while its antibacterial activity will be examined against Gram-positive *Staphylococcus aureus* (*S. aureus*) and Gram-negative *Escherichia coli* (*E. coli*). Comprehensive characterization of AgNP will be carried out using a scanning electron microscope (SEM), Energy-dispersive X-ray (EDX) spectroscopy, dynamic light scattering (DLS), zeta potential and Fourier transform infrared (FTIR) analysis. This study aims to contribute to the development of eco-friendly and sustainable AgNPs using a commonly grown houseplant in Sri Lanka and to provide valuable insights into the potential of Sri Lankan-grown *E. aureum* leaf nanoparticle synthesis. These findings will help us understand how different plant types of the same species with varying phytochemical compositions can produce nanoparticles with varying properties in both environmental and biomedical applications.

2. Experimental

2.1 Sample collection

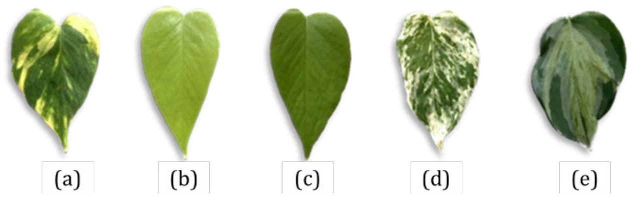

Figure 1. Five leaf types of *E. aureum* and their code names; (a) Golden (GOL), (b) Neon (NEO), (c) Jade (JAD), (d) Marble Queen (MAR), and (e) Manjula (MAN).

Five varieties of *E. aureum* plant leaves were collected from the Wattala and Mount Lavinia areas, Sri Lanka (Figure 1).

2.2 Water-based extraction

The collected samples were shade-dried and crushed using a mortar and pestle. 2 g of dried sample was measured and mixed in 50 mL of distilled water (DW). The beakers were covered in aluminum foil to prevent evaporation and incubated at 60°C for 20 min in the drying oven. The sample was then cooled to room temperature (RT) and filtered using Whatman filter paper no. 01 to obtain the respective water extracts (WE) [23]. WEs were stored in a 50 mL Falcon tube in a refrigerator at 4°C for future experiments.

2.3 Phytochemical analysis in WEs.

Each WE were tested for different phytochemicals such as saponins, tannins, carbohydrates, amino acids, sterols, and alkaloids using standard procedures [55–58].

2.4 Green synthesis of AgNP

A mixture containing 1 mL of each WE and 9 mL of 1 mM silver nitrate solution was incubated at different temperatures and time intervals to synthesize AgNPs; 60°C and 90°C for 15 min, 30 min, 45 min, and 60 min, room temperature (RT) for 24 h [59]. The synthesized AgNPs were stored in the refrigerator at 4°C for future experiments.

2.5 Characterization of MAR_AgNP

2.5.1 UV-Visible spectroscopy

Uv-Visible spectra were recorded on WEs and synthesised AgNPs using UV-1900 spectrophotometer (JENWAY 3605) across 300 nm to 520 nm using DW as the blank.

2.5.2 Scanning electron microscope (SEM) with Energy-dispersive X-ray (EDX) analysis, Dynamic light scattering (DLS) and Zeta potential

An aliquot of MAR_AgNP was centrifuged at 5000 rpm for 2 min. After centrifugation, the supernatant was discarded. The procedure was repeated until a prominent pellet was formed. Finally, the pellet was left to dry at 40°C for 24 h and this was sent to the Sri Lanka Institute of Nanotechnology (SLINTEC) for SEM analysis using HITACHI SU6600 SEM, EDX analysis using Oxford instruments EDX with AZtec software, zeta potential and DLS analysis using Malvern Zetasizer Nano ZS Particle Size Analyser.

2.5.3 Fourier transform infrared (FTIR) spectroscopy analysis

For FTIR analysis using MB300-FTIR spectrometer (ABB, Switzerland) in the mid-infrared region (4000 cm^{-1} to 450 cm^{-1}) at a spectral resolution of 16 cm^{-1} with 64 scans averaged per spectrum. The prepared samples of MAR_ AgNP and MAR_WEs were analysed using the Attenuated Total Reflectance (ATR) method. Spectra were processed using OriginLab® (Massachuserrs, USA) and peak assignments were made by reference to established FTIR literature.

2.6 Dilution of synthesized AgNPs

The synthesized AgNPs of 1 mL at the concentration of 4000 ppm were diluted with 14 mL of DW to obtain the 266 ppm AgNP solution which was used for the following assays.

2.7 Antioxidant assay

2.7.1 Determination of TFC

Into 1 mL WEs and optimized AgNPs, 0.2 mL of 10% aluminum chloride and 1 M potassium acetate was added. This mixture was incubated at RT for 30 min. After incubation, absorbance was measured at 420 nm using DW as the blank [60]. The results were represented as µg of Quercetin (QE) equivalents per 100 g (µg/QE/100 g) using the standard curve.

2.7.2 Determination of TPC

Into 1 mL of WEs and optimized AgNPs, 2 mL of sodium carbonate and 2.5 mL of 10% Folin-Ciocalteu reagent was added. This mixture was incubated at RT for 15 min. After incubation, absorbance was measured at 765 nm using DW as the blank [60]. The results were represented as g of gallic acid equivalents (GAE) per 100 g (g/GAE/100g) using the standard curve.

2.7.3 Determination of TAC

Phosphomolybdenum reagent was prepared using 20 mM sodium phosphate 4 mM ammonium molybdate, and 0.6 M sulfuric acid in ratio of 1:1:1. Into 1 mL of WEs and optimized AgNPs, 1 mL of reagent was added. This mixture was incubated at 95°Cfor 90 min. After incubation, absorbance was measured at 695 nm using DW as the blank [61]. The results were represented as g of ascorbic acid (AA) equivalents per 100 g (g/AA/100g) using the standard curve.

2.8 Photocatalytic degradation of MR dye using MAR_ AgNP under conditions

The curve for 1 mM MR dye was plotted by measuring the absorbance. Then the 1 mL of MR dye was treated with 0.1 mL of 0.2 M sodium borohydride and kept it under the sun light and dark separately. The procedure was repeated with the addition of 1 mL of

4000 ppm and 266 ppm of MAR_AgNP, separately [62]. The absorbance of all experiments was measured at the range of 300 nm to 600 nm using DW as the blank.

2.9 Determination of antibacterial activity

19 g of Muller Hinton agar was dissolved and heated in 50 mL of DW and autoclaved for 15 min at 121°C. After the agar was cooled, it was poured into labeled petri dishes, solidified, and kept under UV light. Inoculums of *E. coli* and *S. aureus* were dissolved in 0.9% saline, and turbidity was compared and adjusted to 0.5% McFarland standard, which was then streaked on respective agar plates using cotton swabs. Three wells were created for S1, S2 and negative control. Into S1 and S2 wells, dried WE and AgNP samples were dissolved in 250 µL of saline and added, whereas positive and negative controls consist of 30 µg gentamicin disks and 0.9% saline water, respectively. Agar plates were incubated for 18 h to 24 h, and the zone of inhibition (ZOI) was measured using a ruler [63].

2.10 Statistical analysis

Antioxidant results were statistically analyzed using Microsoft Excel version (16.73) for one-way ANOVA and SPSS (version 28.0.0.0) for Pearson's correlation.

3. Results and discussion

Research focused on biosynthesis of AgNP has documented promising antibacterial and mosquitocidal activities, cytotoxicity, antitumor properties against human breast cancer cells (MCF-7), synergistic actions with antibiotics, and photocatalytic degradation of dye [64,65]. The purpose of this study is to synthesize AgNP from *E. aureum* leaves, perform comprehensive characterization and evaluate its antibacterial, photocatalytic, and antioxidant properties.

3.1 Green synthesis of *E. aureum* leaf AgNP

The successful synthesis of AgNP involves the bioreduction of Ag^+ ions to Ag atoms, known as the activation phase, facilitated by phytochemicals such as flavonoids, phenols, alkaloids, and polyphenols, which act as reducing agents. The synthesis process also involves a growth phase in which silver ions undergo nucleation, expansion and reduction, Ostwald ripening, and subsequent accumulation of small nanoparticles. The final shape and size of the AgNP is influenced by certain parameters such as concentration of precursor (silver nitrate), temperature, time, and pH [66,67]. The presence of phyto-constituents in the five varieties of *E. aureum* leaves; saponins, alkaloids, tannins, carbohydrates, amino acids, sterols, and triterpenoids (Table 1), which is also reported in research on *E. aureum* leaves phytochemical profiling will act as reducing and capping agents to form stable nanoparticles with specific shape [68–71].

Table 1. Phytochemical test results in *E. aureum* leaves WEs (✓denotes presence; ✗ denotes absence).

Phytochemical	GOL	JAD	NEO	MAR	MAN	Observation
Saponin	✗	✓	✓	✓	✓	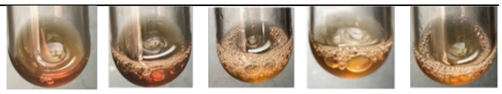
Tannin	✓	✓	✓	✓	✓	
Carbohydrate	✓	✓	✓	✓	✓	
Amino acid	✓	✓	✓	✓	✓	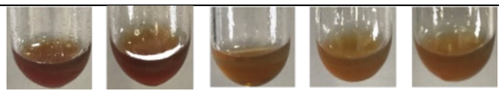
Sterol	✗	✓	✗	✓	✗	
Alkaloid	✓	✓	✓	✓	✓	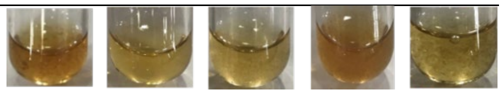

Table 2. Optimization of *E. aureum* leaf silver nanoparticle at 90°C, 60°C, and RT (✓ indicates as synthesized; ✗ indicates as not synthesized).

Sample	RT	60°C				90°C			
ID	24 h	60 min	45 min	30 min	15 min	60 min	45 min	30 min	15 min
JAD	✓	✓	✓	✓	✓	✓	✓	✗	✗
MAR	✗	✓	✓	✓	✓	✗	✓	✗	✗
MAN	✓	✓	✓	✓	✓	✓	✓	✓	✓
NEO	✓	✓	✓	✓	✓	✗	✗	✗	✗
GOL	✗	✓	✓	✓	✓	✗	✗	✓	✗

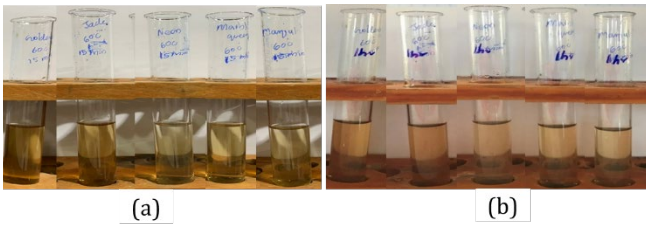

Figure 2. A distinctive colour shift from pale yellow before incubation (a) to dark yellow after incubation, and (b) confirming the formation of silver nanoparticles.

The synthesis of AgNPs is influenced by various factors such as volume of plant extract, concentration of silver precursor (silver nitrate), temperature, pH, and incubation time [72]. Therefore, optimal conditions for *E. aureum* AgNP synthesis should be established by modulating certain parameters. In this study, the influence of temperature and time parameters (Table 2) while keeping the volume of extract and silver nitrate concentration constant was studied.

3.1.1 Visual confirmation of *E. aureum* leaf AgNP

The rapid production and nucleation of AgNPs is generally indicated by the change from light yellow to brownish yellow. The absence of a significant color change during the synthesis of AgNP (Figure 2(a-b)) could be caused due to pH, which directly influences the size and the shape of the AgNP produced, which in turn affects the SPR and the intensity of visible light being reflected [73]. DW was used as the medium for extraction since it was proven to show a high percentage yield of phytochemicals compared to other solutions such as ethanol and ethyl acetate [74].

3.1.2 UV-Vis spectrophotometric confirmation of *E. aureum* leaf AgNP

In addition to confirmation of AgNP synthesis by colour change from yellow to yellow-brown, characteristic absorption peak between 380 nm and 460 nm can also be used. It is due to an optical property of nanoparticles resulting from SPR, which is strongly related to size and dimensions relative to nanoparticles [75]. This states that the free outer electrons present in AgNPs interact with light photons, forming localized plasmons, and oscillate at a specific wavelength of light. The intensities of absorption and scattering are much higher than those of the same particles without plasmonic features [76–78].

The WEs absorbance spectra did not show any peaks between 340 nm to 520 nm. However, the characteristic SPR band of the synthesized nanoparticles appeared at 440 nm (Figure 2(c)), which suggests the complete reduction of elemental silver to AgNPs [23] and AgNPs synthesized at 60°C for 60 min were chosen as the optimized sample. Similar research conducted on AgNP synthesis using leaves of *E. aureum* has reported that at temperatures between 40°C and 60°C, peak absorbance is observed between 411 nm and 462 nm. This research also reports that the optimum conditions for synthesis of *E. aureum* leaf AgNP are 10 mL to 15 mL of plant extract, 0.001 M and 0.1 M silver nitrate concentration, and a temperature of 60°C [22].

In general, an increased temperature will lead to a higher rate of reaction due to kinetic energy, resulting in small AgNPs. However, excessively high temperatures (>80°C/90°C) could lead to the breakdown of plant phytochemicals, which prevents the reduction and stabilization process [79]. Research has reported that as the temperature increases from 50°C to 90°C, there is a decrease in reaction absorbance beyond 70°C [80-82]. Also, research has confirmed that higher incubation time has shown successful nanoparticle synthesis due to the increased number of nanoparticles produced [83]. These findings support the observation of unsuccessful AgNP formation from most leave varieties of *E. aureum* at 90°C in this study (Table 2).

3.2 Characterization of *E. aureum* leaf AgNP

3.2.1 SEM and EDX analysis of *E. aureum* leaf AgNP

The morphology of MAR_AgNP was analyzed using SEM, which provides information on the size and the shape. This analysis reveals a direct correlation between the size and shape of nanoparticles and their attributed properties [84,85]. This analysis confirmed the presence of cubic MAR_AgNPs in the size range of 70 nm and 90 nm (Figure 4). A similar study done using *T. trilobatum* leaf extract, which also belongs to the Araceae family, showed spherical oval-shaped AgNPs with the size range of 70 nm and 90 nm [86]. The size and shape of AgNPs can be controlled by optimizing conditions such as the plant sample, temperature and composition of the extract. Hence, it is expected that *E. aureum* leaf AgNP synthesized at different temperatures might result in different nanoparticle sizes [87].

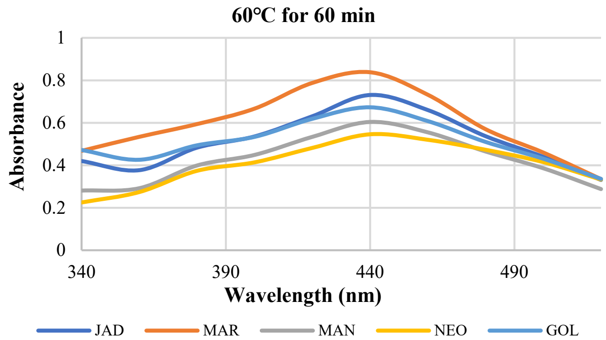

Figure 3. UV–visible spectrum of *E. aureum* leaf silver nanoparticles synthesized at an optimized condition of 60°C for 60 min.

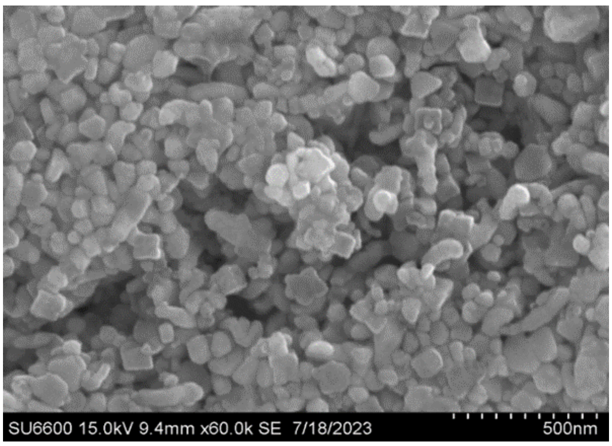

Figure 4. SEM analysis images of MAR_AgNP at 15.0 kV 9.4 mm × 60.0 k at 500 nm.

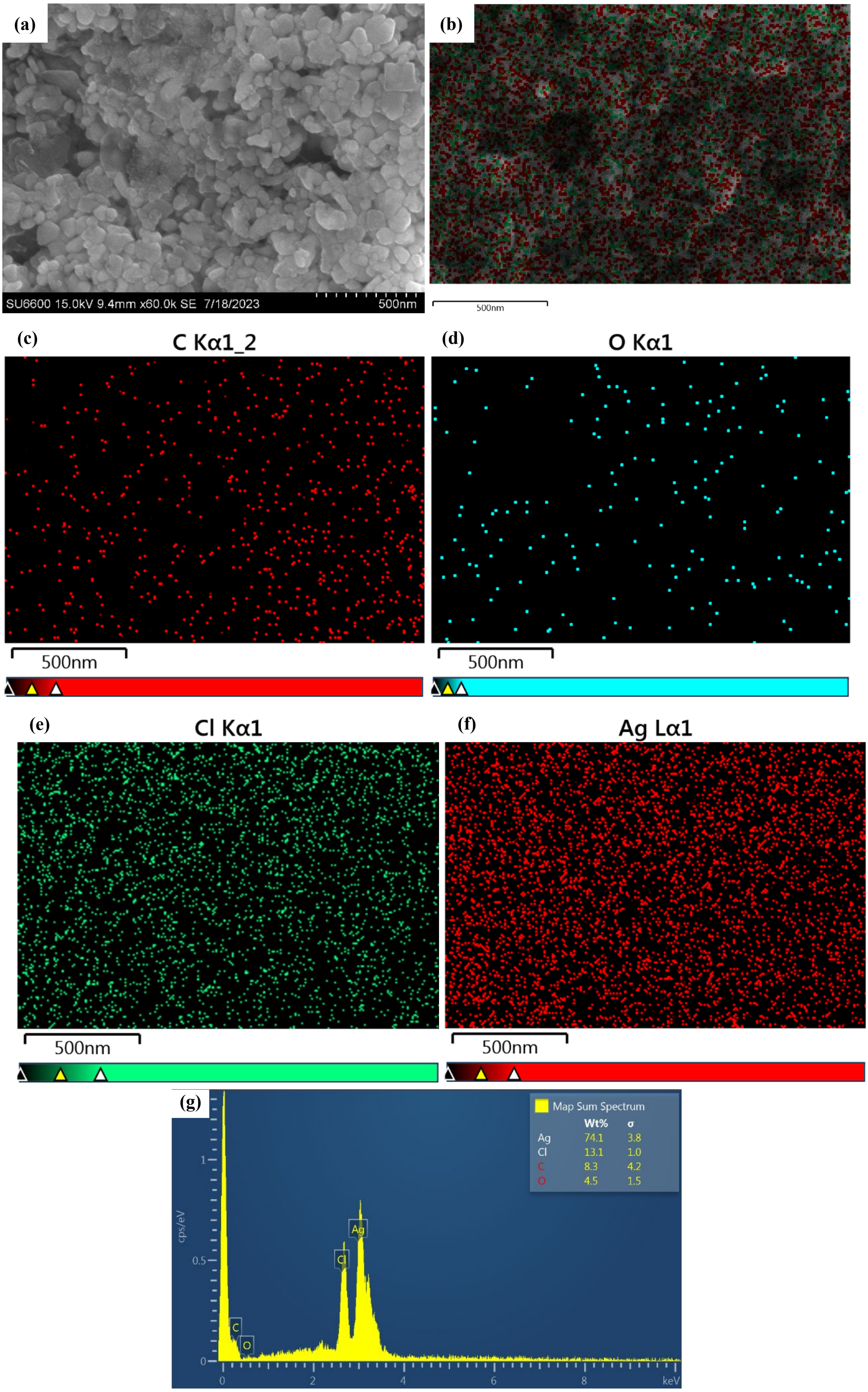

Figure 5. EDX analysis images of MAR_AgNP; (a) SEM image, (b) EDS layered SEM image, (c) C mapping, (d) O mapping, (e) Cl mapping, (f) Ag mapping, and (g) EDS spectrum.

Furthermore, the purity and chemical composition of an analyte such as an AgNP suspension can be obtained by EDX analysis. It gives the silver percentage compared to other chemical elements, which is shown by an optical absorbance peak at 3.7 keV due to the SPR effect [88–90]. EDX analysis of MAR_AgNP shows the presence of silver as cubic shapes (Figure 5(a)), uniform silver dispersion with other elements distribution (Figure 5(b)) and a highest peak at 3keV (74.1%), along with minor peaks for chlorine, carbon and oxygen in the EDX spectrum (Figure 5(g)).

3.2.2 DLS and zeta potential analysis of *E. aureum* leaf AgNP

Zeta potential analysis confirms the colloidal stability of a suspension and DLS analysis confirms the average hydrodynamic size of the AgNP. This is performed by light scattering using Brownian motion of particles to analyze the distribution and hydrodynamic size of the suspension [91]. Additionally, DLS provides a polydispersity index which confirms homogenous suspensions. Zeta potential values more than ±30 mV and polydispersity index less than 0.3 indicate monodispersed stable colloidal suspensions caused by repulsions between individual particles preventing agglomeration in the suspension [92,93].

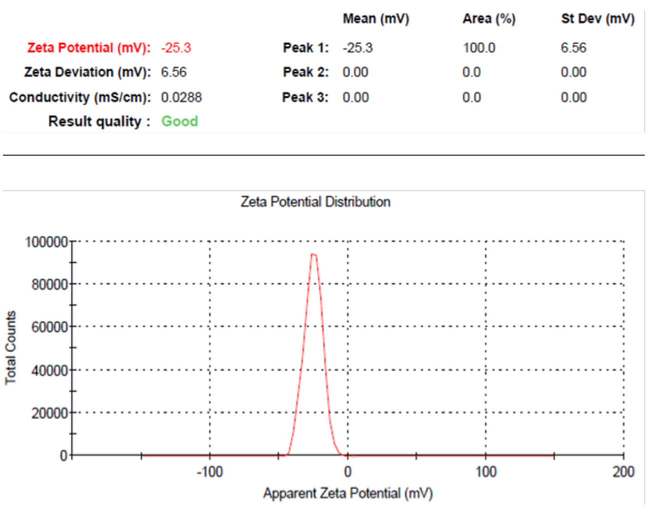

Figure 6. Zeta potential distribution of MAR_AgNP at 60°C for 60 min.

Figure 7. DLS analysis of MAR_AgNP at 60°C for 60 min.

In this study, MAR_AgNP shows zeta potential of –25.3 mV (Figure 6), average hydrodynamic diameter of 74.61 nm and polydispersity index (PDI) value of 0.278 (Figure 7). These results are in close agreement with the SEM analysis results and confirm highly stable and monodispersed AgNP suspension. A recent study conducted on *E. aureum* leaf AgNP has reported high stability with a zeta potential of –34.9 mV [19].

3.2.3 FTIR analysis of *E. aureum* leaf AgNP

FTIR analysis provides information regarding the functional groups present in the analyte; AgNP or WEs. According to the peak sizes obtained, the number of functional groups can be analyzed [94]. FTIR analysis of MAR_AgNP against MAR_WEs demonstrates the presence of various phytochemicals/bio-active compounds which are responsible for AgNP stabilization.

From the FTIR analysis, MAR_WEs showed significant vibration peaks at different wavenumbers such as 3283.1401 cm^{-1} for –OH stretching, 2926.42512 cm^{-1} for C–H stretching, 1451.54589 cm^{-1} for C=C bond stretching, 1310.91787 cm^{-1} for C–N stretching, 1063.96135 cm^{-1} for –COO– (anhydride group) stretching, 2926.42512 cm^{-1} for C–H stretching of aromatics, and 1451.54589 cm^{-1} N–H stretching in the amide linkages of the proteins (Figure 8(a)). These functional groups are responsible for capping and stabilization during AgNP synthesis. The corresponding MAR_AgNP showed primary functional groups indicated by absorption peaks at 1314.78261 cm^{-1}, 1217.3913 cm^{-1}, 1033.04348 cm^{-1}, 820.86957 cm^{-1}, and 765.21739 cm^{-1}. The Ag–O bond vibration was seen at 667.82609 cm^{-1} (Figure 8(b)). When comparison between WE and AgNP, comparatively low absorption peak intensities were visualized and certain peaks shifted between the two [20,22,95].

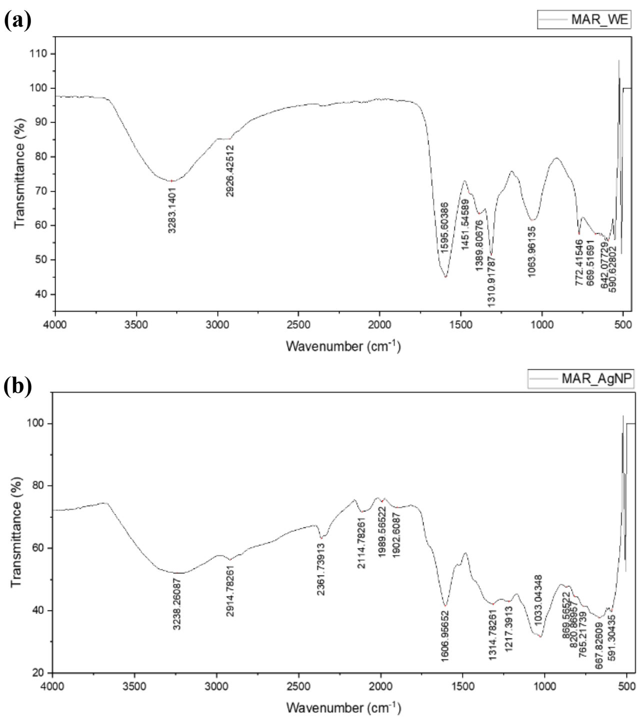

Figure 8. FTIR analysis of; (a) MAR_WE, and (b) MAR_AgNP at 60°C for 60 min.

3.2.4 Band-gap energy analysis of *E. aureum* leaf AgNP.

In addition to morphology, UV-visible absorbance spectra are used to examine the optical characteristics of the AgNPs. Bandgap energy (E) is a key element in determining the conductivity of the nanoparticles. It is the minimum energy required for electrons to move from the valence band (VB) to the conduction band (CB) and is characterized as semiconductors (<3 eV) or insulators (>4 eV) [96]. The optical edge of the synthesized AgNPs was observed at 440 nm. The AgNPs synthesized from this research show semiconductor property with an E value of 2.82 eV, calculated using the Tauc equation, which is also reported by previous research with a value of 2.17 eV [22]. Research has proven that low band-gap energies can be observed when particle size increases due to overlapping orbitals and a decrease in distance between the VB and the CB, which is due to quantum mechanism phenomenon [97]. This is observed from the results of this study, in which particle size distribution is 74.61 nm with a bandgap of 2.82 eV. Additionally, lower values of band gap energies have been reported to show higher antibacterial activity [83].

3.3 Antioxidant activity of *E. aureum* leaf AgNP

The antioxidant potential of five selected varieties of *E. aureum* AgNPs was confirmed by TFC, TPC, and TAC assays. The comparison between WEs and AgNPs was also carried out to emphasize the potential of AgNPs as antioxidants.

The TFC principle relies on the formation of an aluminum chloride ($AlCl_3$)–flavonoid complex with a C-4 keto group and either the C-3 or C-5 hydroxyl group, which can be detected as a yellow colour at 420 nm [98]. AgNPs contained a significantly higher TFC compared to the WEs in the following order: GOL> JAD> MAR > NEO > MAN (Figure 9) with a p-value of 5.91 E-06 ($p<0.05$).

The principle of the TPC assay is the interaction of a redox agent, Folin-Ciocalteu reagent, with polyphenols, which produces a blue chromophore by the reduction of a molybdate-tungstate complex detected at 765 nm [99]. In the following sequence, AgNPs had significantly higher TPC than the WEs. AgNP; JAD > GOL > MAR > MAN > NEO (Figure 10) with a p-value of 4.94E-05 ($p<0.05$). This pattern is due to the electron-donating ability of these phenolic compounds. Additionally, the quinoid compound formed by the oxidation of the phenol group in phenolics can be adsorbed on the surface of nanoparticles, explaining the stabilization of their suspension [100].

The phosphomolybdenum assay is based on the reduction of molybdenum (VI) to molybdenum (V) that leads to the formation of a green complex with maximum absorption of 695 nm [35]. AgNPs had significantly higher TAC compared to the WE in the following order: MAN>JAD>GOL>MAR>NEO (Figure 11) with a p-value of 5.34E-08 ($p<0.05$). This finding is also supported by a previous study [101], who state the antioxidant activity of AgNP may be due to the bioactive compound on the surface of the AgNP, primarily phenols and flavones.

Nevertheless, prior research on the antioxidant potential of *E. aureum* AgNPs and their corresponding WEs has not been carried out to validate the results of this study. To further understand the role of flavonoids and phenols in the antioxidant potential of *E. aureum*, Pearson correlation is performed. This measures the strength of the linear relationship between two variables. In this study, all correlations studied showed strong positive correlation; TAC-TFC = 0.96, TAC-TPC = 0.927 and TFC-TPC = 0.983. These findings also confirmed that the flavonoid compounds that were majorly used to cap the generated AgNPs were more crucial to the stabilization of the form and reduction of the Ag(I) ions than phenols [102].

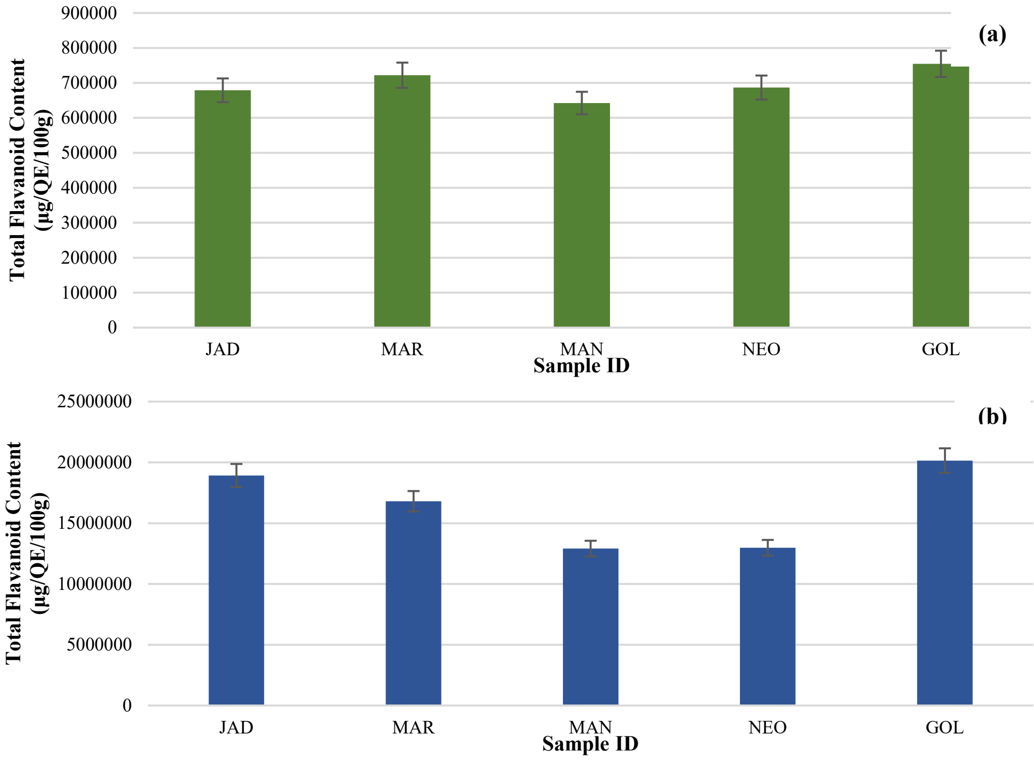

Figure 9. Total flavonoid content of *E. aureum* expressed as µg/QE/100g; (a) leaf water extracts and (b) silver nanoparticles.

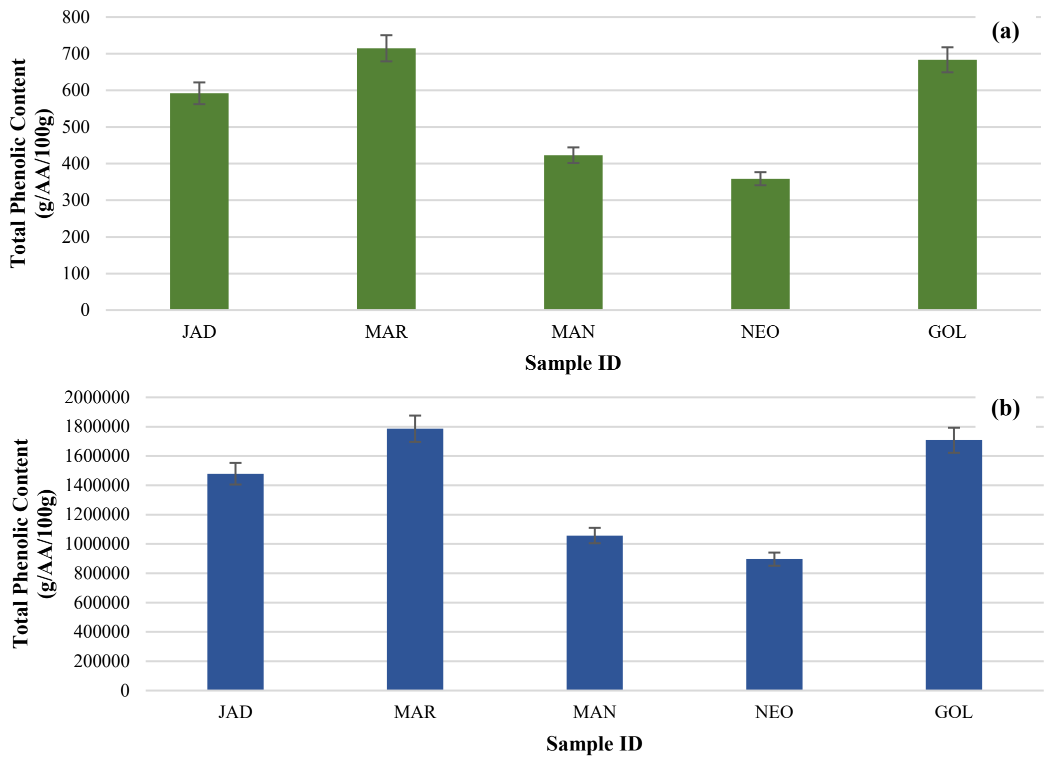

Figure 10. Total phenolic content of *E. aureum* expressed as g/GAE/100g: (a) leaf water extracts and (b) silver nanoparticles.

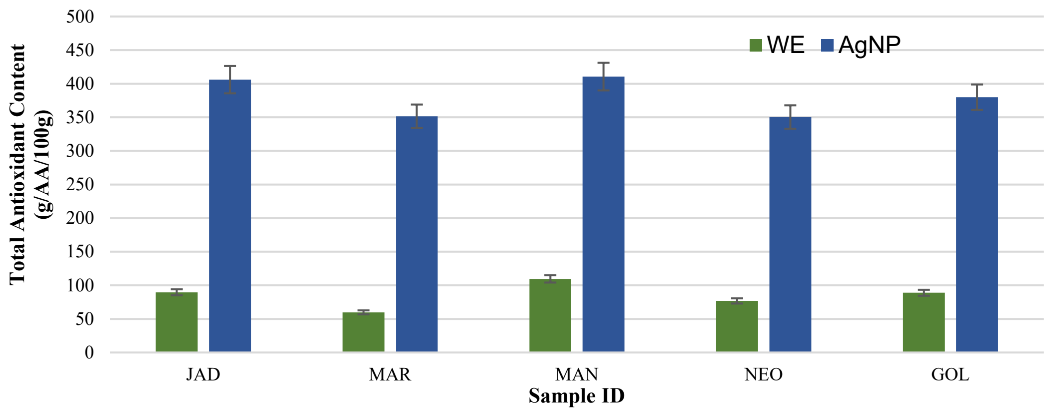

Figure 11. Total antioxidant content of *E. aureum* leaf water extracts and their respective silver nanoparticles expressed as g/AA/100g

3.4 Photocatalytic degradation of *E. aureum* leaf AgNP

Due to the rising concern of wastewater contamination by harmful dyes from industrial effluents, the potential of synthesized AgNPs in degrading these chemicals should be evaluated. The present study evaluated the degradation rates of MAR_AgNP under different conditions. The mechanism of photocatalytic degradation is based on the production of electron holes and radicals that break down azo bonds found in dye molecules. The electrons in the VB of AgNPs become excited under the influence of visible and/or UV radiation and move into the CB. This result in the formation of conduction electrons in the CB and positive holes in the VB [103]. These photo-generated species produce highly reactive radicals capable of degrading azo dyes [104]. These radicals include hydroxyl radicals and superoxide radicals, which attack the azo bonds, hence degrading them into simple, non-toxic fragments like ammonium, carbon dioxide, nitrate, and water [105].

However, the dye is not rapidly degraded by this reaction. Using an electron donor or reducing agent is required to fully facilitate the degradation. The electron donor, sodium borohydride, releases electrons to the dye, which then accepts them as electron acceptor [106]. When AgNP is present in the solution, it aids in the "electron-shuttling" process, which is more effective in transferring electrons from the donor ($NaBH_4$) to the acceptor (dyes). AgNPs' surface is altered by the electron relay mechanism, which is visible as a blue spectral shift in the SPR band [107]. The resonance band of AgNP overlaps the dye's absorption peak as a result of the spectral blue shift. Thus, it is faster and smoother for electrons to flow when a catalyst has an intermediate redox potential between the acceptor and the donor [108]. For this reason, AgNPs have been shown to rapidly break down organic dyes, and AgNPs with band gap energy between 2 eV and 3 eV are reported to show better excitation of electrons in the near-visible region [109,110].

This pattern is also observed in this study; control experiments of MR with just 0.1 mL of 0.2 M sodium borohydride under sunlight and dark conditions yielded no degradation with time (Figure 12(a-b)), and experiments with sunlight and MAR_AgNP showed no degradation (Figure 13(a-b)), whilst the degradation rate increased with the addition of sodium borohydride. In the presence of the catalyst, there is a significant degradation within 75 min in 266 ppm of MAR_AgNP (Figure 14(a)) and complete degradation within 75 min for 4000 ppm of MAR_AgNP (Figure 14(b)).

Although this experiment requires the use of a reducing agent i.e. sodium borohydride, the amount used for the experiment is lower than the amount of AgNP in the system. This behavior is synergistic effect of sodium borohydride and AgNP. Sodium borohydride acts as an essential co-catalyst which gives stability to catalytic surface and provides a continuous flow of electrons [111]. Previous research which has performed photocatalytic degradation of azo dyes using green AgNPs reports that photocatalytic degradation with only sodium borohydride has shown low rates. However, this has increased with the incorporation of AgNPs as sodium borohydride is a reducing agent not a catalyst [112,113].

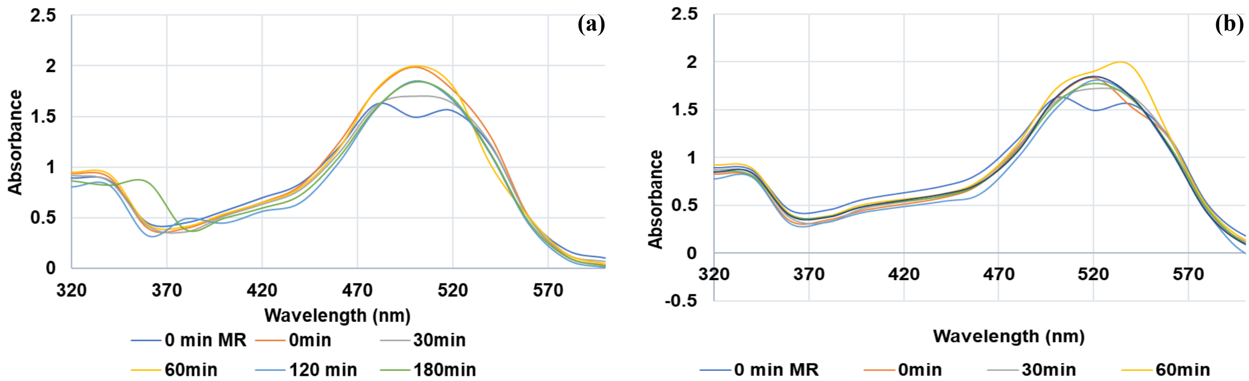

Figure 12. Degradation of 1 mM methyl red dye under different conditions; (a) 0.1 mL of 0.2 mM $NaBH_4$ under sunlight, and (b) 0.1 mL of 0.2 mM $NaBH_4$ under dark condition

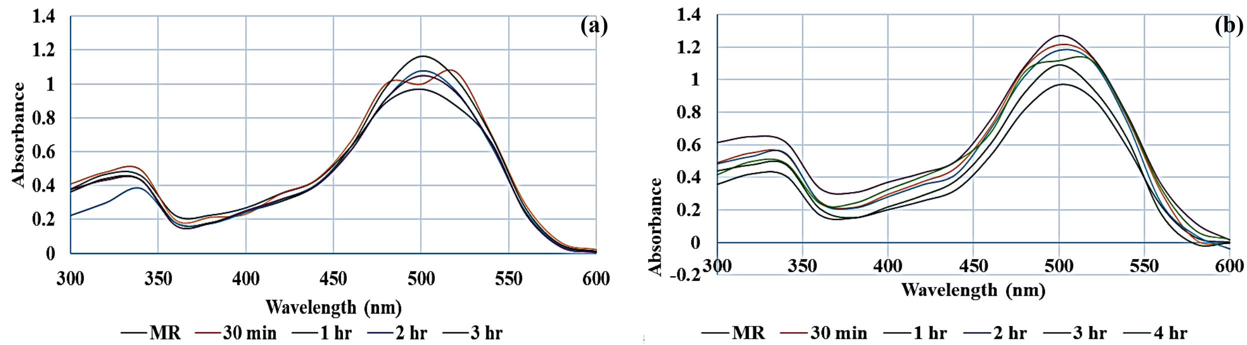

Figure 13. Degradation of 1 mM methyl red dye under different conditions; (a) 1 mL of 266 ppm MAR_AgNP with sunlight, and (b) 1 mL of 4000 ppm MAR_AgNP with sunlight.

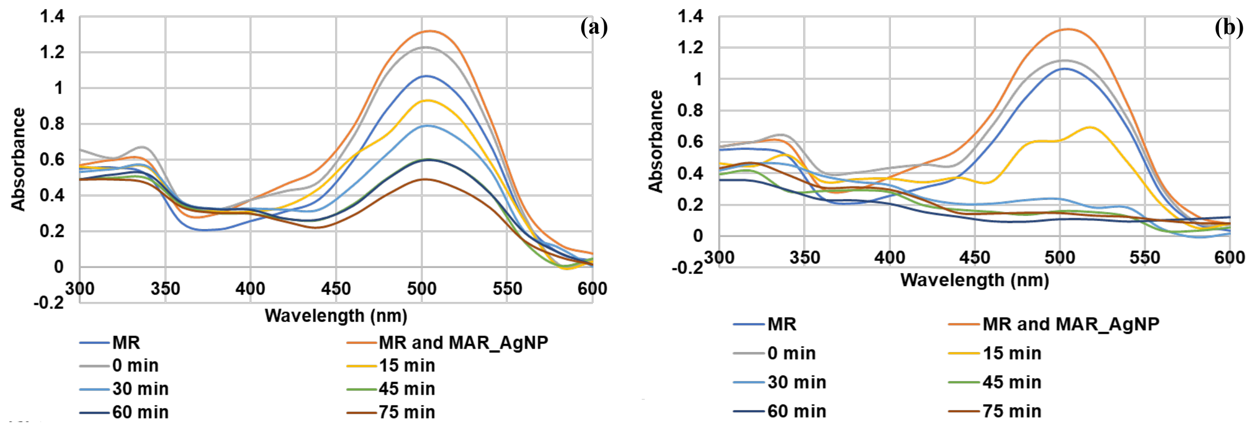

Figure 14. Degradation of 1 mM methyl red dye under different conditions; (a)1 mL of 266 ppm MAR_AgNP in the presence of sunlight and 0.1 mL of 0.2 M sodium borohydride and (b) 1 mL of 4000 ppm MAR_AgNP in the presence of sunlight and 0.1 mL of 0.2 M sodium borohydride.

The reaction kinetics of MR dye degradation in the presence of MAR_AgNP and sodium borohydride under sunlight were also evaluated to determine the rate of reaction. This was evaluated according to Equation (1) following pseudo-1st order reaction kinetics.

$$\text{In}\frac{C_t}{C_0} = kt \quad (1)$$

where k is the rate constant, C_t and C_0 represent the concentration of MR dye at time interval '*t*' and at zero, respectively [107].

The kinetic model shows a good fit at 266 ppm MAR_AgNP concentration (R^2 = 0.9719), which shows that degradation follows pseudo-1st-order. However, at 4000 ppm MAR_AgNP concentration (R^2 = 0.8957), there is a moderate fit, suggesting a deviation to pseudo-1st-order. This deviation can be caused by chemisorption where surface saturation and decrease in active sites occur during the degradation process [114]. Additionally, previous research states the depending on the R^2 value, the degradation reaction with dye concentration lower that the catalyst concentration follows pseudo-1st-order and the reaction will follow pseudo-2nd-order when dye gets absorbed onto the AgNP surface. These findings correlate to the observation in this research experiment [115–117].

The rate constant, *k*, was determined using the linear regression slope, which showed a value of k = 0.1948 min^{-1} for 4000 ppm MAR_AgNP (Figure 15(a)) and a value of k = 0.0752 for 266 ppm MAR_ AgNP (Figure 15(b)). These results highlight that at a higher concentration of *E. aureum* AgNP, faster degradation is obtained. The photocatalytic degradation capacity is also influenced by several factors, such as dye concentration, surface area, number of active sites, and light penetration [118]. Modulation of these factors will show different rates of reactions, as observed in this study. The photocatalytic potential of *E. aureum* AgNP has not been conducted; however, *E. aureum* zinc oxide nanoparticles have shown 57.6% degradation of Congo red dye, which has increased to 80.82% after optimization of conditions [26], vanadium pentoxide needle-shaped nanorods synthesised using *E. aureum* have shown excellent photocatalytic degradation of methyl blue dye [119], morphology-Modified Bi_2WO_6 Nanoparticles using *E. aureum* has reported near complete degradation of Victoria Blue and Auramine O dyes [120], and magnesium oxide nanoparticles – composite synthesized using *E. aureum* leaf reported excellent degradation capacity of 91% for Crystal violet and Reactive black [121]. These findings highlight the potential of *E. aureum* leaf to act as an efficient photocatalytic degradation capacity against azo dyes.

3.5 Antibacterial activity of *E. aureum* leaf AgNP.

Antibacterial activity of AgNP is proposed to have several mechanisms. The interaction of the negatively charged bacterial cell membrane and positively charged nanoparticles caused damage to the cell membrane and increased its permeability. This is followed by the production of reactive oxygen species, which will deactivate important bacterial respiratory enzymes, interact with DNA and prevent its replication, denature proteins, and also lead to oxidative stress. Ultimately, these mechanisms lead to bacterial cell death [122,123]. This antibacterial potential of AgNP can differ depending on Gram-positive and Gram-negative bacteria. Gram-positive bacteria have a thick peptidoglycan cell wall, while Gram-negative bacteria have a thin peptidoglycan cell wall and outer membrane composed of porins and lipopolysaccharide. This additional feature in Gram-negative bacteria promotes the entry of AgNP through porins and penetration. On the other hand, in Gram-positive bacteria, incubation with AgNP leads to destruction of the β-1,4-glycoside bond between the polymers found in the peptidoglycan layer, which causes cleavage of the cell wall and release of N-acetylglucosamine. Other research has documented that the acid-base reactions between AgNPs and gram-negative bacterial cells can also cause cell death [124]. In addition, since the Gram-positive bacterial cell wall is negatively charged, it tends to bind with more Ag^+, lowering the interaction of AgNPs with the plasma membrane and protecting it from ROS generated by AgNPs. Another factor that influences the potential of antibacterial activity by AgNPs is their size and shape. Small-sized AgNPs have a higher surface-to-volume ratio, allowing them to penetrate the cell membrane easily, while large-sized AgNPs cause cell membrane damage [125,126].

To study the antibacterial potential of *E. aureum* AgNPs, model microorganisms were used: *E. coli* (Gram-negative bacteria) and *S. aureus* (Gram-positive bacteria). A higher antibacterial activity against *E. coli* and *S. aureus* was shown by all AgNPs and some WEs in the following order: *E. coli* AgNP: GOL>MAR=MAN=NEO>JAD, *E. coli* WE: GOL>MAR=MAN>JAD, *S. aureus* AgNP: MAN>GOL>JAD>MAR=NEO, and *S. aureus* WE: MAR>JAD>NEO=GOL (Table 3). Comparison of ZOIs between *E. coli* and *S. aureus* in this study shows a higher antibacterial activity against *E. coli.*

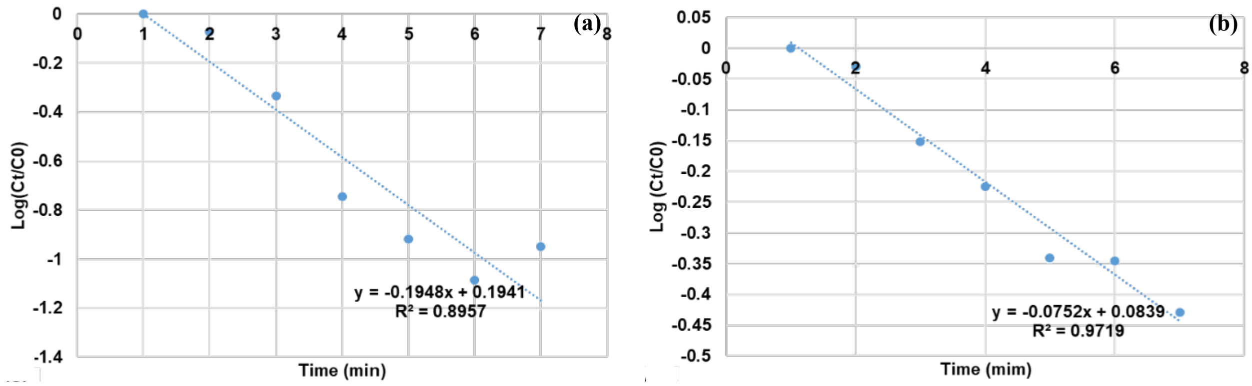

Figure 15. Reaction kinetics plot of degradation of methyl red in the presence of (a) 4000 ppm MAR_AgNP and sodium borohydride under sunlight and (b) 266 ppm MAR_AgNP and sodium borohydride under sunlight.

Table 3. ZOI against *E.coli* and *S. aureus* for silver nanoparticles and their respective water extracts.

Sample ID	*E.coli*		*S. aureus*	
	Average ZOI/cm	Positive ZOI/cm	Average ZOI/cm	Positive ZOI/cm
JAD_AgNP	1.45	2.6	1.2	2.8
MAR_AgNP	1.5	2.7	1	2.7
MAN_AgNP	1.5	2.7	1.75	2.7
NEO_AgNP	1.5	2.5	1	2.6
GOL_AgNP	1.75	2.5	1.25	2.75
JAD_WE	1.2	2.6	1.1	2.5
MAR_WE	1.5	2.6	1.6	2.6
MAN_WE	1.5	2.5	0	0
NEO_WE	0	0	1	2.8
GOL_WE	2	2	1	2.7

4. Conclusion

This study explores a novel and green synthesis approach to synthesize AgNPs using *E. aureum* leaf extract. The current research proves that WEs obtained from the selected five varieties of *E. aureum* leaves can be useful in AgNP synthesis, which has not yet been carried out for this purpose. The optimized synthesis condition was determined to be at 60°C for 60 min. The SEM analysis confirmed cubic MAR_AgNP of 70 nm to 90 nm which was also confirmed by DLS (74.61 nm average diameter), EDX confirmed high presence of Ag, zeta potential confirmed high stability of –25.3 mV, and FTIR confirmed the presence of several functional groups required for AgNP synthesis. The conductivity study showed semiconductors property (E = 2.82 eV). The antioxidant activity was confirmed by higher TFC, TPC, and TAC in AgNPs than WEs. *E. aureum* AgNPs displayed a higher rate of 0.1948 min^{-1} MR dye degradation at 4000 ppm and addition of sodium borohydride along with a lower rate at 266 ppm (k =0.0752 min^{-1}). These findings suggest promising photocatalytic potential of *E. aureum* leaf AgNPs, which can be used in environmental remediation applications. Nevertheless, more investigation is required to achieve optimal degradation conditions for optimal effectiveness. The current study displayed a significant effect on bacterial growth inhibition against *S. aureus* and *E. coli.* These findings on characterization, antioxidant capacity, photocatalytic capacity, and antibacterial capacity highlight the potential of *E. aureum* leaf AgNPs for various applications such as medicinal, agricultural, and wastewater treatment. However, further research should focus on understanding the mechanisms behind these properties, optimizing the synthesis process and evaluation of safety profile on animal models to enhance the performance of *E. aureum* leaf AgNPs for practical use.

Acknowledgements

The authors would like to acknowledge the Business Management School (BMS) campus for funding, Sri Lanka Institute of Nanotechnology (SLINTEC) for the analysis using the Hitachi SU6600 SEM, EDX analysis using Oxford instruments EDX with AZtec software, zeta potential and DLS analysis using Malvern Zetasizer Nano ZS Particle Size Analyser and Institute of Chemistry Ceylon (IChemC), Sri Lanka for the analysis using the MB300-FTIR spectrometer.

References

[1] A. Singh, D. Jain, M. K. Upadhyay, N. Khandelwal, and H. N. Verma, "Green synthesis of silver nanoparticles using argemone mexicana leaf extract and evaluation of their antimicrobial activities," *Digest Journal of Nanomaterials and Biostructures*, vol. 5, no. 2, pp. 483–489, 2010.

[2] P. Nagarajan, D. T. Raj, K. Y. Gowri, S. A. Siddiqua, and D. J. P. Innocent, "Synthesis of silver phyto nanoparticles and their antibacterial efficacy," *Digest Journal of Nanomaterials and Biostructures*, vol. 5, no. 1, pp. 185–189, 2010.

[3] C. Tiloke, A. Phulukdaree, and A. A. Chuturgoon, "The Chemotherapeutic potential of gold nanoparticles against human carcinomas: A review," *Nanoarchitectonics for Smart Delivery and Drug Targeting*, pp. 783–811, 2016.

[4] A. Dhaka, S. C. Mali, S. Sharma, and R. Trivedi, "A review on biological synthesis of silver nanoparticles and their potential applications," *Results in chemistry*, vol. 6, pp. 101108–101108, 2023.

[5] M. F. Khan, A. H. Ansari, M. Hameedullah, E. Ahmad, F. M. Husain, Q. Zia, U. Baig, M. R. Zaheer, M. M. Alam, A. M. Khan, Z. A. AlOthman, I. Ahmad, G. M. Ashraf, and G. Aliev "Sol-gel synthesis of thorn-like ZnO nanoparticles endorsing mechanical stirring effect and their antimicrobial activities: Potential role as nano-antibiotics," *Scientific Reports*, vol. 6, no. 1, 2016.

[6] A.-L. Grün, W. Manz, Y. L. Lohl. F. Meier, S. Straskraba, C. Jost, R. Drexel, and C. Emmerling, "Impact of silver nanoparticles (AgNP) on soil microbial community depending on functionalization, concentration, exposure time, and soil texture," *Environmental Sciences Europe*, vol. 31, Art. no. 15, 2019,

[7] D. Bharathi, and V. Bhuvaneshwari, "Evaluation of the cytotoxic and antioxidant activity of phyto-synthesized silver nanoparticles using cassia angustifolia flowers," *BioNanoScience*, vol. 9, no. 1, pp. 155–163, 2018.

[8] S. H. Lee, and B.-H. Jun, "Silver Nanoparticles: Synthesis and application for nanomedicine," *International Journal of Molecular Sciences*, vol. 20, no. 4, p. 865, 2019.

[9] M. Shah, D. Fawcett, S. Sharma, S. Tripathy, and G. Poinern, "Green synthesis of metallic nanoparticles via biological entities," *Materials*, vol. 8, no. 11, pp. 7278–7308, 2015.

[10] S. S. Shankar, A. Rai, A. Ahmad, and M. Sastry, "Rapid synthesis of Au, Ag, and bimetallic Au core–Ag shell nanoparticles using Neem (Azadirachta indica) leaf broth," *Journal of Colloid and Interface Science*, vol. 275, no. 2, pp. 496–502, 2004

[11] A. Rónavári, N. Igaz, D. I. Adamecz, B. Szerencses, C. Molnar, Z. Konya, I. Pfeiffer, and M. Kiricsi, "Green silver and gold nanoparticles: Biological synthesis approaches and potentials for biomedical applications," *Molecules*, vol. 26, no. 4, 2021

[12] A. K. Jha, K. Prasad, K. Prasad, and A. R. Kulkarni, "Plant system: Nature's nanofactory," *Colloids and Surfaces B: Biointerfaces*, vol. 73, no. 2, pp. 219–223, 2009.

[13] J. Chen, "Three new cultivars of pothos (Epipremnum aureum)," *HortScience*, vol. 59, no. 12, pp. 1736–1739, 2024

[14] T. Attanayake, Y. M. H. M. H. Dasanayaka, H. K. L. Dilshan H. Buddhika, S. Gamage, P. A. S. C. Wickramasinghe, C. R. Dayarathna, and H. M. P. C. Kumarihami, "Stimulatory effect of indole – 3 – butyric acid and rooting media on adventitious rooting in epipremnum aureum 'Marble Queen' stem cuttings," *Indonesian Journal of Applied Research*, vol. 4, no. 3, pp. 193–208, 2023.

[15] A. Liyanage, F. Nashath, K. A. S. Karunanayake, and A. N. M. Mubarak, "Modified coir dust media elevate the production of superior quality epipremnum aureum .l plantlets derived from stem cuttings," *Sri Lankan Journal of Technology*, vol. 02, no. Special Issue, pp. 34–38, 2021.

[16] D. Moodley, Ş. Procheş, and J. R. U. Wilson, "Assessing and managing the threat posed by Epipremnum aureum in South Africa," *South African Journal of Botany*, vol. 109, pp. 178–188, 2017.

[17] N. Srivasatava, S. Shwarupa, and S. Bhagyawant, "Comparative study on the anti-termite, antimicrobial and antioxidant activity of leaf and root extracts of Pothosaurea (Epipremnum aureum L.)," *Journal of Pharmaceutical Research and Clinical Practice*, vol. 1, no. 2, pp. 1–11, 2011.

[18] A. Meshram, and N. Srivastava, "Phytochemical screening and in vitro antioxidant potential of methanolic extract of Epipremnum aureum (Linden and Andre) G. S. Bunting," *International Journal of Pharmaceutical Research & Allied Sciences*, vol. 5, no. 2, pp. 1–6, 2016.

[19] S. Ravichandran, S. Ramalingam, G. Senthilkumar, M. Paulpandi, and R. Saravanan, "Cytotoxic and apoptotic effects of epipremnum aureum-mediated silver nanoparticles on MCF-7 breast cancer cells," *Cell Biochemistry and Biophysics*, vol. 84, 2025.

[20] Y. Ale, S. Rana, V. Jakhmola, K. Kumar, R. S. Rana, D. Rawat, and N. Nidhi, "Antiproliferative activity of green process synthesized epipremnum aureum silver nanoparticles against breast cancer Mcf-7 cells," *Biomedical and Pharmacology Journal*, vol. 17, no. 3, pp. 1795–1806, 2024.

[21] M. Merino-Treviño, A. B. Morales-Cepeda, H. Peraza-Vázquez, and E. Onofre-Bustamante, "Plants with silver nanoparticles to improve electrical conductivity: An innovative approach in biology," *International Journal of Environmental Science and Technology*, vol. 22, no. 7, pp. 5181–5192, 2024.

[22] R. K. Chaudhari, and P. S. Shrivastav, "Sustainable synthesis of silver nanoparticles using epipremnum aureum leaf extract: Application in copper ion sensing and antimicrobial activity," *Asian Journal of Chemistry*, vol. 36, no. 9, pp. 2120–2128, 2024.

[23] Komal, Sonia, S. Kukreti, and M. Kaushik, "Exploring the potential of environment friendly silver nanoparticles for DNA interaction: Physicochemical approach," *Journal of Photochemistry and Photobiology B: Biology*, vol. 194, pp. 158–165, 2019.

[24] T. Sinha, S. H. S. A. Kumar Satapathy, B. P. Singh, V. H. Singh, A. Kumar, P. S. Gupta, and S. Atteri, "Synthesis and characterization of copper oxide nanoparticles using epipremnum aureum extract: Biological activities, and environmental applications," *International Journal of Environmental Sciences*, vol. 11, no. 6s, pp. 356–375, 2025.

[25] Kajal, P. Devi, S. Thakur, and K. Jeet, "Green synthesis of zinc oxide nanoparticles using epipremnum aureum extract: Characterization, biological activities, and environmental applications," *Journal of Neonatal Surgery*, vol. 14, no. 23S, pp. 709–728, 2025.

[26] R. S. Brishti, Md. A. Habib, M. H. Ara, K. Md. R. Karim, Md. K. Islam, J. Naime, Md. M. H. Rumon, and Md. A. R. Khan, "Green synthesis of ZnO NPs using aqueous extract of Epipremnum aureum leave: Photocatalytic degradation of Congo red," *Results in chemistry*, vol. 7, pp. 101441–101441, 2024.

[27] V. P. Reddy, "Oxidative stress in health and disease," *Biomedicines*, vol. 11, no. 11, pp. 2925–2925, 2023.

[28] L. Azeez, A. Lateef, and S. A. Adebisi, "Silver nanoparticles (AgNPs) biosynthesized using pod extract of Cola nitida enhances antioxidant activity and phytochemical composition of Amaranthus caudatus Linn," *Applied Nanoscience*, vol. 7, no. 1–2, pp. 59–66, 2017.

[29] Z. Li, H. Jiang, C. Xu, and L. Gu, "A review: Using nanoparticles to enhance absorption and bioavailability of phenolic phytochemicals," *Food Hydrocolloids*, vol. 43, pp. 153–164, 2015.

[30] M. C. Lite, R. R. Constantinescu, E. C. Tanasescu, A. Kuncser, C. Romanitan, D. E. Mihaiescu, I. Lacatusu, and N. Badea, "Phytochemical synthesis of silver nanoparticles and their antimicrobial investigation on cotton and wool textiles," *Materials*, vol. 16, no. 11, pp. 3924–3924, 2023.

[31] Z. Bedlovičová, I. Strapáč, M. Baláž, and A. Salayová, "A brief overview on antioxidant activity determination of silver nanoparticles," *Molecules*, vol. 25, no. 14, p. 3191, 2020.

[32] G. Singhal, R. Bhavesh, K. Kasariya, A. R. Sharma, and R. P. Singh, "Biosynthesis of silver nanoparticles using Ocimum sanctum (Tulsi) leaf extract and screening its antimicrobial activity," *Journal of Nanoparticle Research*, vol. 13, no. 7, pp. 2981–2988, 2011.

[33] J. N. Russell, and C. K. Yost, "Alternative, environmentally conscious approaches for removing antibiotics from wastewater treatment systems," *Chemosphere*, vol. 263, p. 128177, 2021.

[34] G. R. Rudramurthy, M. K. Swamy, U. R. Sinniah, and A. Ghasemzadeh, "Nanoparticles: Alternatives against drug-resistant pathogenic microbes," *Molecules*, vol. 21, no. 7, p. 836, 2016.

[35] H. F. Hammodi , I. H. Rashid , and A. G. Oraibi , "Green biosynthesis, identification and characterization of ag and zn nano-

particles using ivy (Epipremnum Aureum) plant extract," *Plant Archives*, vol. 19, pp. 959–965, 2019.

[36] S. Gevorgyan, R. Schubert, S. Falke, K. Lorenzen, K. Trchounian, and C. Betzel, "Structural characterization and antibacterial activity of silver nanoparticles synthesized using a low-molecular-weight Royal Jelly extract," *Scientific Reports*, vol. 12, no. 1, p. 14077, 2022.

[37] A. Gupta, S. Mumtaz, C.-H. Li, I. Hussain, and V. M. Rotello, "Combatting antibiotic-resistant bacteria using nanomaterials," *Chemical Society Reviews*, vol. 48, no. 2, pp. 415–427, 2019.

[38] G. B. Singh, A. Vinayak, G. Mudgal, and K. K. Kesari, "Azo dye bioremediation: An interdisciplinary path to sustainable fashion," *Environmental Technology & Innovation*, vol. 36, p. 103832, 2024.

[39] F. A. Batzias, and D. K. Sidiras, "Dye adsorption by prehydrolysed beech sawdust in batch and fixed-bed systems," *Bioresource Technology*, vol. 98, no. 6, pp. 1208–1217, 2007.

[40] G. Buitrón, M. Quezada, and G. Moreno, "Aerobic degradation of the azo dye acid red 151 in a sequencing batch biofilter," *Bioresource Technology*, vol. 92, no. 2, pp. 143–149, 2004.

[41] N. Baig, S. Shetty, M. S. Moustafa, S. Al-Mousawi, and B. Alameddine, "Selective removal of toxic organic dyes using Tröger base-containing sulfone copolymers made from a metal-free thiol-yne click reaction followed by oxidation," *RSC Advances*, vol. 11, no. 34, pp. 21170–21178, 2021.

[42] L. R. S. Pinheiro, D. G. Gradíssimo, L. P. Xavier, and A. V. Santos, "Degradation of Azo Dyes: Bacterial potential for bio-remediation," *Sustainability*, vol. 14, no. 3, p. 1510, 2022.

[43] A. Strebel, M. Behringer, H. Hilbig, A. Machner, and B. Helmreich, "Anionic azo dyes and their removal from textile wastewater through adsorption by various adsorbents: A critical review," *Frontiers in environmental engineering*, vol. 3, 2024.

[44] W. Wang, F. Lin, B. Yan, Z. Cheng, G. Chen, M. Kuang, C. Yang, and L. Hou, "The role of seashell wastes in TiO_2/Seashell composites: Photocatalytic degradation of methylene blue dye under sunlight," *Environmental Research*, vol. 188, p. 109831, 2020.

[45] M. Ajaz, S. Shakeel, and A. Rehman, "Microbial use for azo dye degradation—a strategy for dye bioremediation," *International Microbiology*, vol. 23, no. 2, pp. 149–159, 2019.

[46] A. C. R. Ngo and D. Tischler, "Microbial degradation of azo dyes: Approaches and prospects for a hazard-free conversion by microorganisms," *International Journal of Environmental Research and Public Health*, vol. 19, no. 8, p. 4740, 2022.

[47] B. Lellis, C. Z. Fávaro-Polonio, J. A. Pamphile, and J. C. Polonio, "Effects of textile dyes on health and the environment and bioremediation potential of living organisms," *Biotechnology Research and Innovation*, vol. 3, no. 2, pp. 275–290, 2019.

[48] F. P. van der Zee, and S. Villaverde, "Combined anaerobic–aerobic treatment of azo dyes—A short review of bioreactor studies," *Water Research*, vol. 39, no. 8, pp. 1425–1440, 2005.

[49] S. Vishal, A. Sarvesvaron, M. Keethana, H. S. Reddy, and A. B. Ponnusami, "Degradation of wastewater by advanced oxidation processes using green synthesised CuO nanoparticles," *Journal of metals, materials and minerals* , vol. 36, no. 1, p. e2467, 2026.

[50] Y. Tangjaideborisut, S. Shanmugam, S. Boonyuen, G. Siva, P. Yugala, J. C. Juan, C. Phanawansombat, A. Pitintharangkul, S. Vasantharaj, P. Pungpo, and P. N. Nakorn, "Eco-friendly synthesis of flower-like hierarchical structure of CuO NPs for advancing photocatalytic efficiency and antibacterial applications," *Journal of Metals, Materials and Minerals*, vol. 35, no. 3, p. e2351, 2025.

[51] P. Sonthongphithak, C. Muangnapoh, C. Ratanatawanate, T. E-Kobon, A. Piyasaengthong, P. Hongsachart, M. Sriuttha, N. Sengkhamparn, A. C. T. A. Dhanapal, and K. Wittayanarakul, "Biosynthesis of zinc oxide nanoparticles using water hyacinth extracts: Characterization, evaluation of antimicrobial and dye removal," *Journal of Metals, Materials and Minerals*, vol. 34, no. 2, pp. 1979–1979, 2024.

[52] G. Govindasamy, and A. B. Ponnusami, "Facile bio-synthesis of cerium oxide nanoparticles, characterization and their photo-catalytic potential in the degradation of real tannery wastewater," *Journal of Metals, Materials and Minerals*, vol. 35, no. 4, p. e2405, 2025.

[53] C. K. Githala, S. Raj, A. Dhaka, S. N. Mali, and R. Trivedi, "Phyto-fabrication of silver nanoparticles and their catalytic dye degradation and antifungal efficacy," *Frontiers in Chemistry*, vol. 10, 2022.

[54] M. B. Sumi, A. Devadiga, V. K. Shetty , and S. M. B., "Solar photocatalytically active, engineered silver nanoparticle synthesis using aqueous extract of mesocarp of Cocos nucifera (red spicata dwarf)," *Journal of Experimental Nanoscience*, vol. 12, no. 1, pp. 14–32, 2016.

[55] M. Yadav and K. K. Saravanan, "Phytochemical analysis and antioxidant potential of rhizome extracts of curcuma amada roxb and curcuma caesia roxb," *Journal of Drug Delivery and Therapeutics*, vol. 9, no. 5, pp. 123–126, 2019.

[56] P. Singh, Y.-J. Kim, D. Zhang, and D.-C. Yang, "Biological synthesis of nanoparticles from plants and microorganisms," *Trends in Biotechnology*, vol. 34, no. 7, pp. 588–599, 2016.

[57] A. A. Oladipupo, "Comparative study of photochemical and proximate analysis of breadfruit seeds, leaves and barks," *IOSR Journal of Applied Chemistry*, vol. 7, no. 5, pp. 86–89, 2014.

[58] M. Gupta, S. Thakur, A. Sharma, and S. Gupta, "Qualitative and quantitative analysis of phytochemicals and pharmacological value of some dye yielding medicinal plants," *Oriental Journal Of Chemistry*, vol. 29, no. 2, pp. 475–481, 2013.

[59] J. Y. Song, and B. S. Kim, "Rapid biological synthesis of silver nanoparticles using plant leaf extracts," *Bioprocess and Biosystems Engineering*, vol. 32, no. 1, pp. 79–84, 2008.

[60] Y. Martono, F. F. Yanuarsih, N. R. Aminu, and J. Muninggar, "Fractionation and determination of phenolic and flavonoid compound from Moringa oleifera leaves," *Journal of Physics: Conference Series*, vol. 1307, no. 1, p. 012014, 2019.

[61] N. B. Sadeer, D. Montesano, S. Albrizio, G. Zengin, and M. F. Mahomoodally, "The versatility of antioxidant assays in food science and safety—chemistry, applications, strengths, and limitations," *Antioxidants*, vol. 9, no. 8, p. 709, 2020.

[62] A. Roy, and N. Bharadvaja, "Silver nanoparticle synthesis from Plumbago zeylanicaand its dye degradation activity," *Bioinspired,*

Biomimetic and Nanobiomaterials, vol. 8, no. 2, pp. 130–140, 2019.

[63] M. Kandiah, and K. N. Chandrasekaran, "Green synthesis of silver nanoparticles using catharanthus roseus flower extracts and the determination of their antioxidant, antimicrobial, and photocatalytic activity," *Journal of Nanotechnology*, vol. 2021, pp. 1–18, 2021.

[64] M. Sathiyaraj, D. Elumalai, V. Rajendran, M. Hemavathi, K. Ashok, M. Babu, U. Monisha, S. Poonguzhali, S. Punithavalli, and G. Abirami, "Biosynthesis, characterization, and multifaceted applications of Elytraria acaulis synthesized silver and gold nanoparticles: Anticancer, antibacterial, larvicidal, and photocatalytic activities," *Journal of Photochemistry and Photobiology B: Biology*, vol. 263, p. 113102, 2025.

[65] A. E. El-Ansary, A. A. A. Omran, H. I. Mohamed, and O. M. El-Mahdy, "Green synthesized silver nanoparticles mediated by Fusarium nygamai isolate AJTYC1: Characterizations, antioxidant, antimicrobial, anticancer, and photocatalytic activities and cytogenetic effects," *Environmental Science and Pollution Research*, vol. 30, 2023.

[66] K. Deka, R. D. Nongbet, K. Das, P. Saikia, S. Kaur, A. Talukder, and B. Thakuria, "Understanding the mechanism underlying the green synthesis of metallic nanoparticles using plant extract(s) with special reference to silver, gold, copper and zinc oxide nanoparticles," *Hybrid Advances*, vol. 9, no. 1, p. 100399, 2025.

[67] F. Eker, E. Akdaşçi, H. Duman, M. Bechelany, and S. Karav, "Green synthesis of silver nanoparticles using plant extracts: A comprehensive review of physicochemical properties and multifunctional applications," *International Journal of Molecular Sciences*, vol. 26, no. 13, p. 6222, 2025.

[68] S. Ferdousi, M. S. Alam, E. Ahmmed, R. S. Brishti, and Md. A. R. Khan, "Catalytic reduction of benzaldehyde using green synthesized cuprous oxide nanoparticles," *Results in Chemistry*, vol. 13, p. 101935, 2024.

[69] Ritu, K. K. Verma, A. Das, and P. Chandra, "Phytochemical-based synthesis of silver nanoparticle: Mechanism and potential applications," *BioNanoScience*, vol. 13, no. 3, 2023.

[70] S. Bawazeer, A. Rauf, S. U. A. Shah, A. M. Shawky, Y. S. Al-Awthan, O. S. Bahattab, G. Uddin, J. Sabir, and M. A. El-Esawi, "Green synthesis of silver nanoparticles using *Tropaeolum majus*: Phytochemical screening and antibacterial studies," *Green Processing and Synthesis*, vol. 10, no. 1, pp. 85–94, 2021.

[71] A. Meshram, A. Kumar, and N. Srivastava, "Gas chromatography-mass spectrometry (GC-MS) analysis of alkaloids isolated from epipremnum aureum (linden and andre) bunting," *International Journal of Pharma Sciences and Research (IJPSR)*, vol. 6, no. 2, pp. 337–342, 2015.

[72] N. S. Alharbi, N. S. Alsubhi, and A. I. Felimban, "Green synthesis of silver nanoparticles using medicinal plants: Characterization and application," *Journal of Radiation Research and Applied Sciences*, vol. 15, no. 3, pp. 109–124, 2022.

[73] N. Liaqat, N. Jahan, K. Rahman, T. Anwar, and H. Qureshi, "Green synthesized silver nanoparticles: Optimization, characterization, antimicrobial activity, and cytotoxicity study by hemolysis assay," *Frontiers in Chemistry*, vol. 10, 2022.

[74] D. A. Ondigo, W. L. L. Munyendo, D. Andala, A. O. Maima, J. M. Mosweta, and K. Odhiambo, "Enhancement of antibacterial activity through phyto-fabrication of silver nanoparticles with *Ficus thonningii* aqueous extracts," *IET Nanobiotechnol*, vol. 16, no. 7–8, pp. 250–258, 2022.

[75] A. M. Fayaz, K. Balaji, P. T. Kalaichelvan, and R. Venkatesan, "Fungal based synthesis of silver nanoparticles—An effect of temperature on the size of particles," *Colloids and Surfaces B: Biointerfaces*, vol. 74, no. 1, pp. 123–126, 2009.

[76] R. K. Singh, A. Ramanathan, A. Hegde, and V. Kumblekar, "'Exploring the green science of silver nanoparticles: The process of nano-scale sculpting,'" *Plasmonics*, vol. 20, 2025.

[77] M. Rycenga, C. M. Cobley, J. Zeng, W. Li, C. H. Moran, Q. Zhang, D. Qin, and Y. Xia, "Controlling the synthesis and assembly of silver nanostructures for plasmonic applications," *Chemical Reviews*, vol. 111, no. 6, pp. 3669–3712, 2011.

[78] J. M. Ashraf, M. A. Ansari, H. M. Khan, M. A. Alzohairy, and I. Choi, "Green synthesis of silver nanoparticles and characterization of their inhibitory effects on AGEs formation using biophysical techniques," *Scientific Reports*, vol. 6, no. 1, 2016.

[79] R. M. D. L. Cruz-Puma, J. Vega-Chacón, V. R. Jauja-Ccana, J. E. L. Villa, and A. L. Rosa-Toro, "Green synthesis and characterization of silver nanoparticles using grape stalk extract," *Journal of Molecular Liquids*, vol. 403, pp. 124927–124927, 2024.

[80] N. H. Ibrahim, G. M. Taha, N. Sh, and M. A. Moghazy, "Green synthesis of silver nanoparticles and its environmental sensor ability to some heavy metals," *BMC chemistry*, vol. 18, no. 1, 2024.

[81] Y. Gou, R. Zhou, X. Ye, S. Gao, and X. Li, "Highly efficient in vitro biosynthesis of silver nanoparticles using Lysinibacillus sphaericus MR-1 and their characterization," *Science and Technology of Advanced Materials*, vol. 16, no. 1, pp. 015004–015004, 2015.

[82] M. I. Khan, M. N. Akhtar, N. Ashraf, J. Najeeb, H. Munir, T. I. Awan, M. B. Tahir, and M. R. Kabli, "Green synthesis of magnesium oxide nanoparticles using Dalbergia sissoo extract for photocatalytic activity and antibacterial efficacy," *Applied Nanoscience*, vol. 10, no. 7, pp. 2351–2364, 2020.

[83] M. R. Shaik, M. Khan, M. Kuniyil, A. Al-Warthan, H. Z. Alkhathlan, M. R. H. Siddiqui, J. P. Shaik, A. Ahamed, A. Mahmood, M. Khan, and S. F. Adil, "Plant-extract-assisted green synthesis of silver nanoparticles using *Origanum Vulgare L.* extract and their microbicidal activities," *Sustainability*, vol. 10, no. 4, p. 913, 2018.

[84] N. Joudeh, and D. Linke, "Nanoparticle classification, physicochemical properties, characterization, and applications: A comprehensive review for biologists," *Journal of Nanobiotechnology*, vol. 20, no. 1, 2022.

[85] B. Sadeghi, and F. Gholamhoseinpoor, "A study on the stability and green synthesis of silver nanoparticles using Ziziphora tenuior (Zt) extract at room temperature," *Spectrochimica Acta Part A: Molecular and Biomolecular Spectroscopy*, vol. 134, no. 5, pp. 310–315, 2015.

[86] S. Ghosh, and S. N. Sinha, "Untying the antimicrobial and

antioxidant potential of silver nanoparticles fabricated from Typhonium trilobatum (L.) Schott," *Plant Nano Biology*, vol. 10, p. 100113, 2024.

[87] V. Kumar, and S. K. Yadav, "Synthesis of different-sized silver nanoparticles by simply varying reaction conditions with leaf extracts of Bauhinia variegata L.," *IET Nanobiotechnology*, vol. 6, no. 1, p. 1, 2012.

[88] M. Goudarzi, N. Mir, M. Mousavi-Kamazani, S. Bagheri, and M. Salavati-Niasari, "Biosynthesis and characterization of silver nanoparticles prepared from two novel natural precursors by facile thermal decomposition methods," *Scientific Reports*, vol. 6, no. 1, 2016.

[89] A. B. Chavan, S. Goyal, and A. M. Patel, "Formulation of silver nanoparticles using gymnema sylvestre leaf extract and in-vitro anti-diabetic activity," *Journal of Pharmaceutical Research International*, vol. 34, no. 7A, pp. 39–49, 2022.

[90] J. R. Manullang, R. A. Nugroho, M. Rohmah, R. Rudiato, and A. Qorysuchi, "Plant-extract-mediated biosynthesis of silver nanoparticles using Eleutherine americana bulb extract and its characterization," *Nusantara Bioscience*, vol. 13, no. 2, 2021.

[91] A. M. Eid, S. E.-D. Hassan, M. F. Hamza, S. Selim, M. S. Almuhayawi, M. H. Alruhaili, M. K. Tarabulsi, M. K. Nagshabandi, and A. Fouda, "Photocatalytic, antimicrobial, and cytotoxic efficacy of biogenic silver nanoparticles fabricated by bacillus amyloliquefaciens," *Catalysts*, vol. 14, no. 7, pp. 419–419, 2024.

[92] A. K. Alzubaidi, W. J. Al-Kaabi, A. A. Ali, S. Albukhaty, H. Al-Karagoly, G. M. Sulaiman, M. Asiri, and Y. Khane, "Green synthesis and characterization of silver nanoparticles using flaxseed extract and evaluation of their antibacterial and antioxidant activities," *Applied sciences*, vol. 13, no. 4, pp. 2182–2182, 2023.

[93] A. P. Z. de Melo, M. V. de. O. B. Maciel, W. G. Sganzerla, A. da. R. Almeida, R. D. de Armas, M. H. Machado, C. G. da Rosa, M. R. Nunes, F. C. Bertoldi, and P. L. M. Barreto, "Antibacterial activity, morphology, and physicochemical stability of bio-synthesized silver nanoparticles using thyme (Thymus vulgaris) essential oil," *Materials Research Express*, vol. 7, no. 1, pp. 015087–015087, 2020.

[94] S. Jaast, and A. Grewal, "Green synthesis of silver nanoparticles, characterization and evaluation of their photocatalytic dye degradation activity," *Current Research in Green and Sustainable Chemistry*, vol. 4, p. 100195, 2021.

[95] K. Jyoti, M. Baunthiyal, and A. Singh, "Characterization of silver nanoparticles synthesized using Urtica dioica Linn. leaves and their synergistic effects with antibiotics," *Journal of Radiation Research and Applied Sciences*, vol. 9, no. 3, pp. 217–227, 2016.

[96] D. Sundeep, T. V. Kumar, P. S. S. Rao, R. V. S. S. N. Ravikumar, and A. G. Krishna, "Green synthesis and characterization of Ag nanoparticles from Mangifera indica leaves for dental restoration and antibacterial applications," *Progress in Biomaterials*, vol. 6, no. 1–2, pp. 57–66, 2017.

[97] A. K. Roddu, A. W. Wahab, A. Ahmad, and P. Taba, "Green-route synthesis and characterization of the silver nanoparticles resulted by bio-reduction process," *Journal of Physics: Conference Series*, vol. 1341, no. 3, p. 032004, 2019.

[98] H. M. Ilmi, B. Elya, and R. Handayani, "Association between total phenol and flavonoid contents in artocarpus heterophyllus (Jackfruit) bark and leaf extracts and lipoxygenase inhibition," *International Journal of Applied Pharmaceutics*, vol. 12, no. 1, pp. 252–256, 2020.

[99] A. Blainski, G. Lopes, and J. de Mello, "Application and analysis of the folin ciocalteu method for the determination of the total phenolic content from Limonium Brasiliense L.," *Molecules*, vol. 18, no. 6, pp. 6852–6865, 2013.

[100] W. Wang, Q. Chen, C. Jiang, D. Yang, X. Liu, and S. Xu, "One-step synthesis of biocompatible gold nanoparticles using gallic acid in the presence of poly-(N-vinyl-2-pyrrolidone)," *Colloids and Surfaces A: Physicochemical and Engineering Aspects*, vol. 301, no. 1–3, pp. 73–79, 2007.

[101] B. Selvaraj, K. Subramanian, G. Suresh, R. Balasubramanian, and M. s. N. Sundari, "Phytosynthesis of silver nanoparticles using hygrophila auriculata leaf extract and assessment of their antibacterial and antioxidant properties," *International Journal of Applied Pharmaceutics*, vol. 10, no. 6, p. 112, 2018.

[102] M. Sharifi-Rad, P. Pohl, and F. Epifano, "Phytofabrication of silver nanoparticles (AgNPs) with pharmaceutical capabilities using otostegia persica (Burm.) boiss. leaf extract," *Nanomaterials*, vol. 11, no. 4, p. 1045, 2021.

[103] T. Sinha, M. Ahmaruzzaman, and A. Bhattacharjee, "A simple approach for the synthesis of silver nanoparticles and their application as a catalyst for the photodegradation of methyl violet 6B dye under solar irradiation," *Journal of Environmental Chemical Engineering*, vol. 2, no. 4, pp. 2269–2279, 2014.

[104] W. A. Shaikh, S. Chakraborty, and R. U. Islam, "Photocatalytic degradation of rhodamine B under UV irradiation using Shorea robusta leaf extract-mediated bio-synthesized silver nanoparticles," *International Journal of Environmental Science and Technology*, vol. 17, no. 4, pp. 2059–2072, 2019.

[105] K. Tahir, S. Nazir, B. Li, A. U. Khan, Z. U. H. Khan, A. Ahmad, and F. U. Khan, "An efficient photo catalytic activity of green synthesized silver nanoparticles using Salvadora persica stem extract," *Separation and Purification Technology*, vol. 150, pp. 316–324, 2015.

[106] T. Varadavenkatesan, R. Vinayagam, and R. Selvaraj, "Green synthesis and structural characterization of silver nanoparticles synthesized using the pod extract of Clitoria ternatea and its application towards dye degradation," *Materials Today: Proceedings*, 2019.

[107] N. Pradhan, A. Pal, and T. Pal, "Silver nanoparticle catalyzed reduction of aromatic nitro compounds," *Colloids and Surfaces A: Physicochemical and Engineering Aspects*, vol. 196, no. 2–3, pp. 247–257, 2002.

[108] R. M. Tripathi, N. Kumar, A. Shrivastav, P. Singh, and B. R. Shrivastav, "Catalytic activity of biogenic silver nanoparticles synthesized by Ficus panda leaf extract," *Journal of Molecular Catalysis B: Enzymatic*, vol. 96, pp. 75–80, 2013.

[109] A. B. Siddique, M. A. Shaheen, A.Abbas, Y. Zaman, M. A. Bratty, A. Najmi, A. Hanbashi, M. Mustaqeem, H. A. Alhazmi, Z. U.

Rehman, K. Zoghebi, and H. M. A. Amin, "Thermodynamic and kinetic insights into azo dyes photocatalytic degradation on biogenically synthesized ZnO nanoparticles and their antibacterial potential," *Heliyon*, vol. 10, no. 23, p. e40679, 2024.

[110] R. E. Adam, G. Pozina, M. Willander, and O. Nur, "Synthesis of ZnO nanoparticles by co-precipitation method for solar driven photodegradation of Congo red dye at different pH," *Photonics and Nanostructures - Fundamentals and Applications*, vol. 32, pp. 11–18, 2018.

[111] P. Nathawat, M. Sahu, and M. Ganguly, "Role of sodium borohydride as a co-catalyst for nanoparticle-induced degradation of toxic dyes in aquatic systems," *Nanoscale Advances*, vol. 8, no. 6, pp. 1791–1816, 2026.

[112] P. K. Pandey, J. Sarkar, and S. Srivastava, "Catalytic dye degradation of textile dye methylene blue by using silver nanoparticles fabricated by sustainable approach," *Engineering Proceedings*, vol. 37, no. 1, 2023.

[113] S. C. Paul, S. Bhowmik, M. R. Nath, Md. S. Islam, S. K. Paul, J. Neazi, T. S. B. Monir, S. Dewanjee, and M. A. Salam, "Silver nanoparticles synthesis in a green approach: size dependent catalytic degradation of cationic and anionic dyes," *Oriental Journal of Chemistry*, vol. 36, no. 03, pp. 353–360, 2020.

[114] A. Mohammadi, and A. R. Karimi, "Methylene blue removal using surface-modified TiO_2 nanoparticles: A comparative study on adsorption and photocatalytic degradation," *Journal of Water and Environmental Nanotechnology*, vol. 2, no. 2, pp. 118–128, 2017.

[115] G. A. K. Nabi, S. Hussain, M. Ullah, S. Azizi, I. Kamika, and M. Maaza, "Kinetic investigation of photocatalytic degradation of methyl orange dye using Mg-doped Ag_2O nanoparticle," *Scientifica*, vol. 2026, no. 1, 2026.

[116] M. Alamzeb, S. Faryad, I. Ullah, J. Hussain, and W. N. Setzer, "Photocatalytic degradation of brilliant blue dye under solar light irradiation: an insight into mechanistic, kinetics, mineralization and scavenging studies," *Journal of Fluorescence*, vol. 30, no. 10, 2025.

[117] P. Sharma, S. Kar, M. Sahu, and M. Ganguly, "Copper-based nanoparticles for the removal of the crystal violet dye *via* degradation and adsorption: A comparative account," *RSC Advances*, vol. 15, no. 34, pp. 27995–28020, 2025.

[118] Z. Khalid, A. Ali, A. B. Siddique, Y. Zaman, M. F. Sibtain, A. Abbas, M. M. Alam, and M. S. Alwethaynani, "*Causonis trifolia*-based green synthesis of multifunctional silver nanoparticles for dual sensing of mercury and ferric ions, photocatalysis, and biomedical applications," *RSC Advances*, vol. 15, no. 21, pp. 16879–16893, 2025.

[119] V. Dubey, K. D. Parikh, D. H. Vyas, R. J. Jadav, H. E. A. Mohamed, and S. Ghotekar, "Insights into the photocatalytic and supercapacitor performance of V_2O_5 nanorods synthesized by green synthetic approach using Epipremnum aureum leaves extract," *Biomass Conversion and Biorefinery*, vol. 15, no. 6, pp. 8755–8770, 2024.

[120] K. Hemkumar, G. Vignesh, and P. Anitha, "Investigation of morphology-modified Bi_2WO_6 nanoparticles with surface plasmon resonance effect for the enhanced photocatalytic degradation of organic dyes: Toxicity Estimation and in silico studies," *ACS Applied Nano Materials*, vol. 7, no. 18, pp. 21284–21295, 2024.

[121] B. Murugesan, D. Madhan, V. Devabharathi, D. S. Kumar, T. A. Christy, S. Surendhiran, A. Balamurugan, and Y. A. S. Khadar, "Phytofabrication of MgO NPs wrapped on exfoliated g-C_3N_4 for anti-oxidant, antimicrobial degradation of toxic contaminants in water bodies," *Inorganic Chemistry Communications*, vol. 170, p. 113427, 2024.

[122] E. O. Mikhailova, "Green silver nanoparticles: an antibacterial mechanism," *Antibiotics*, vol. 14, no. 1, pp. 5–5, 2024.

[123] K. Bhatt, A. Kongor, M. Atharb, and V. Jain, "New views on the ingenious applications of Ag nanoparticles as a sensor for antibiotic detection and as a potent antimicrobial agent," *Journal of Metals, Materials and Minerals*, vol. 31, no. 3, pp. 1–9, 2021.

[124] S. Prabhu, and E. K. Poulose, "Silver nanoparticles: mechanism of antimicrobial action, synthesis, medical applications, and toxicity effects," *International Nano Letters*, vol. 2, no. 1, 2012.

[125] G. Chinnasamy, S. Chandrasekharan, T. W. Koh, and S. Bhatnagar, "Synthesis, characterization, antibacterial and wound healing efficacy of silver nanoparticles from azadirachta indica," *Frontiers in Microbiology*, vol. 12, 2021.

[126] A. Menichetti, A. Mavridi-Printezi, D. Mordini, and M. Montalti, "Effect of size, shape and surface functionalization on the antibacterial activity of silver nanoparticles," *Journal of Functional Biomaterials*, vol. 14, no. 5, p. 244, 2023.